

Plasma Polymer Membranes from Hexafluoroethane/Hydrogen Mixtures for Separation of Oxygen and Nitrogen

F. HUBER,¹ J. SPRINGER,¹ M. MUHLER²

¹Technische Universität Berlin, Institut für Technische Chemie, Fachgebiet Makromolekulare Chemie, Straße des 17. Juni 124, D-10623 Berlin, Germany

²Fritz-Haber-Institut der Max-Planck-Gesellschaft, Faradayweg 4-6, D-14195 Berlin, Germany

Received 15 May 1996; accepted 8 July 1996

ABSTRACT: Thin plasma polymer layers were produced employing feed mixtures of hexafluoroethane and hydrogen in an rf parallel-plate reactor. The layers are intended for use in membrane-based separation of oxygen and nitrogen. The hexafluoroethane-to-hydrogen mixture ratio was varied over a wide range, whereas all other process parameters (power, pressure, substrate temperature, and total gas flow) were held constant. The plasma polymers were examined by scanning electron microscopy, X-ray analysis, quantitative elemental analysis, and X-ray photoelectron spectroscopy. Permeability coefficients of oxygen and nitrogen and selectivities of the pure gases were determined. Pinhole-free plasma polymer films containing different amounts of fluorine, carbon, and hydrogen were formed. The distributions of fluorine and hydrogen in the products reflect their distributions in the feed gas. Traces of oxygen in some of the polymers are explained by the reaction of trapped radicals with atmospheric oxygen on the samples' exposure to air. Fluorine-containing carbon moieties such as CF₃, CF₂, and CF, and carbon moieties with fluorine atoms exclusively in secondary positions are present. A method of calculating crosslink density using the analytical data is described. The oxygen permeability coefficient and the selectivity of the plasma polymers increase as the hexafluoroethane content of the feed gas is raised. This behavior is attributed to growing solubility selectivity as a result of the rising fluorine content of the polymers. Maximum selectivity amounts to 3.4 at an oxygen permeability coefficient of 21 Barrer. © 1997 John Wiley & Sons, Inc. *J Appl Polym Sci* **63**: 1517–1526, 1997

Key words: gas separation membranes; thin film technology; plasma polymerization; separation of oxygen and nitrogen; solubility-type selectivity

INTRODUCTION

Membrane-based gas separation for the production of oxygen- or nitrogen-enriched air is becoming more and more technically attractive. Concerning profitability today it already outperforms cryogenic fractionation of air and pressure swing adsorption in the small output range.¹ To be viable in commercial application, a membrane must

exhibit both a high selectivity, which characterizes its separation performance, and a high permeability to the desired component of a mixture, thus enabling high flow rates. Unfortunately, selectivity and permeability seem to be inversely proportional in most cases and hence, to achieve sufficient flow rates, the membranes must be sufficiently thin. For air separation nonporous polymer layers are most suitable, but though there exist numerous methods of production of thin polymer films,² usually it is still difficult to make them simultaneously pinhole-free and ultrathin.

Plasma polymerization permits the deposition

Correspondence to: J. Springer.

© 1997 John Wiley & Sons, Inc. CCC 0021-8995/97/121517-10

of ultrathin pinhole-free layers in a process entirely different from conventional polymerization reactions.³⁻⁶ In the first reaction step, the molecules of an organic gas exposed to a glow discharge undergo electron impact and subsequent fragmentation into radicals. Several ensuing steps, in particular the combination of carbon-bearing radicals, lead to the generation of larger molecules. After repeated fragmentation and combination, a highly crosslinked plasma polymer that adheres to any surface present in the reaction chamber is formed. A practically unlimited number of gases and gas mixtures may be employed as feed, in this way allowing the production of depositions with nearly tailor-made separation properties.

Gas permeation through nonporous polymer membranes⁷ (to which further discussion will be restricted) is caused by a difference in partial pressure between the upstream and the downstream sides of a membrane. Application of a gas pressure onto the upstream side entails the sorption of the gas molecules at the membrane surface, which is followed by diffusion of the dissolved molecules through the membrane to the downstream side, where the penetrant is finally released from solution. The steady-state flow rate dn/dt is given by

$$\frac{dn}{dt} = PA \frac{\Delta p}{l}$$

where P denotes the permeability coefficient, A is the membrane area, Δp is the pressure difference, and l is the thickness of the separation layer. The permeability coefficient is given by

$$P = DS$$

where D is the diffusion coefficient and S is the sorption coefficient. The ratio of the permeability coefficients of two different gases A and B in the same membrane material is termed "selectivity":

$$\alpha = \frac{P_A}{P_B}$$

From experience, the sorption coefficient of oxygen is known to rise with the fluorine content of the solvent.⁸ On the other hand, the diffusion coefficient of any gas will increase when the energy of polymer-chain separation is reduced, since the gas molecules diffuse through interchain chan-

nels which are frequently created and destroyed by thermal activation.^{9,10}

This paper deals with fluorine-containing plasma polymers produced from different hexafluoroethane/hydrogen mixtures and their applicability in membrane-based air separation. Oxygen and nitrogen permeation rates through dense polymer layers deposited onto porous aluminium oxide were determined by measuring the increase of pressure in a constant volume. The thickness of the layers was identified by scanning electron microscopy (SEM), which was also used to study the quality of the depositions, and selectivities and permeability coefficients were calculated. Data obtained from X-ray analysis, elemental analysis, and X-ray photoelectron spectroscopy (XPS) will serve to elucidate the separation properties of the plasma polymer membranes.

EXPERIMENTAL

Materials

Any ultrathin gas separation layer must be supported by a mechanically stable substrate to withstand the applied pressure difference. The substrate ought not to affect the permeability of the whole composite membrane, and, in the present case it must also be chemically inert under the conditions of the plasma. Microporous, ceramic materials seem to satisfy these demands best. To allow covering of the support with a pinhole-free plasma polymer film, the pore diameter should be about an order of magnitude smaller than the film thickness. Anodisc 47 aluminium oxide membranes (Anotec Separations Ltd., Banbury, U.K.) with a pore diameter of 20 nm exhibit the required microporous structure. Nevertheless, since these membranes are only 60 μm in thickness, they must be fixed onto a second support to provide sufficient mechanical stability to the composite. Porous Robu sinter glass plates (supplied by Berliner Normalschliff Gerätebau, Berlin, Germany) usually employed in vacuum filtration and having a thickness of 2.5 mm, were found to be well-suited. Thus, any of the composite membranes examined in this study consisted of a first dense layer of plasma polymer, a second layer of microporous aluminium oxide, and a third layer of porous sinter glass.

To remove hydrocarbons and dust from the aluminium oxide substrates, they were rinsed with tetrachloromethane before coating.

Hexafluoroethane employed as feed gas of the plasma process was of 99.998% purity; hydrogen had a purity of 99.999%. Oxygen used for permeability measurements was of 99.9% purity, and nitrogen of 99.999% purity.

Plasma Polymerization

The glow discharges were generated in a self-constructed parallel-plate reactor system operating at 27.12 MHz, which has been described in detail previously.¹¹ The reaction chamber consists of two parallel aluminium plates separated by a cylindrical glass tube (inside diameter 232 mm; height 30 mm) making up the reaction volume. The round upper plate is the excitation electrode and serves as the lid of the chamber. The lower plate is both the grounded electrode and the bottom of the chamber, having apertures for admission and exhaustion of the feed gas. Under the bottom plate a disk-shaped tube run through by water is installed, thus permitting regulation of the temperature by means of a thermostat. For experiment, the round aluminium-oxide membranes are fixed by an annular holder onto the middle of the bottom plate, where they are coated with polymer, homogeneously covering an area 40 mm in diameter.

The feed gas is introduced into the reaction chamber, passing mass flow controllers and conveyed using a rotary pump. Between the reaction chamber and the pump a throttle valve is installed, thus allowing adjustment of operating pressure independently of gas flow rate and pump performance.

Feed composition was varied using mixtures of hexafluoroethane and hydrogen at 30 different volume ratios between 1 : 2 and approximately 6 : 1. Hydrogen must be admixed to the feed to catch atomic fluorine, which would etch the deposition and possibly prevent, or at least hinder, polymerization. Except for the feed composition, all other process parameters were held constant (plasma power 16.5 W; operating pressure 1.1 mbar; substrate temperature 20°C; total flow rate 20 ml[STP]/min). In each case, the polymerization time was 2 h. Power, pressure, and total flow rate were chosen, concerning any feed composition, to

- enable ignition of the plasma,
- ensure stability of the discharge,
- give rise to the deposition of coherent polymer films, and
- avoid polymer powder formation.

SEM

SEM was performed to determine the layer thickness and the quality of the plasma polymer depositions, and especially to check whether they are pinhole-free. The plasma polymer-coated aluminium-oxide membranes were broken and their fracture surface perpendicular to the polymer layer surface was micrographed. To achieve good electric conductivity the samples were sputtered with gold before examination. The micrographs were taken on a Hitachi S-2700 scanning electron microscope.

X-ray Analysis

The content of carbon and fluorine in the plasma polymers was measured with a Kevex Delta 5 X-ray analyzer. Electron energy was 10 keV, corresponding to an information depth of about 2 μm . The analyzed area of the sample amounted to around 100 μm^2 . For better electric conductivity the samples were coated with a thin carbon layer (thickness of around 10 nm). Because the sum of element percentages has never been exactly 100%, ratios of fluorine-to-carbon molar content are given, which are more reliable.

Quantitative Elemental Analysis

Quantitative carbon and hydrogen elemental analysis was carried out on a Perkin Elmer Series II CHNS/O Analyzer 2400. The polymer film cannot be detached mechanically from the aluminium-oxide support, and for that reason the deposition was pulverized in a mortar together with the substrate and explored in this state. Since only the molar ratio of hydrogen to carbon was extracted from the analysis, the aluminium oxide from the substrate material did not falsify the data. Quantities of around 0.5 mg of plasma polymer were enough for examination.

X-ray Photoelectron Spectroscopy

CF_3 , CF_2 , and CF structural features, and carbon bound only to carbon and hydrogen but with fluorine substituents in secondary positions (β -fluorine), were quantified by means of XPS. The spectra were recorded in a modified Leybold LHS 12 MCD system with MgK_α radiation. The analyzer was operated at 108 eV pass energy yielding a resolution of 1.2 eV at Au 4 $f_{7/2}$ level (binding energy 84.0 eV). Charging was corrected using the

F1s level (binding energy 689 eV) as internal standard.¹² Quantitative data analysis was performed by subtracting stepped backgrounds and using empirical cross-sections.¹² Mixed Gaussian/Lorentzian product functions were used for the nonlinear least-squares curve fitting. The position, the height, the full width at half maximum, and the Gaussian/Lorentzian percentage of the product functions were varied until correspondence of the fit with the observed spectra was achieved.

Permeability Measurements

Permeation rates for pure oxygen and nitrogen were determined by applying a constant gas pressure onto the upstream side of the membranes and measuring the increase of pressure in a closed volume at the downstream side. The permeation rates were converted into permeability coefficients by arithmetical elimination of pressure difference, membrane area, and the thickness of the polymer layer. Upstream pressure was 2 bar, downstream pressure was near zero, and temperature was constant at 25°C. Before each experiment, the membranes were degassed under vacuum. A detailed description of the procedure and the apparatus has been published elsewhere.¹³ The permeation cell especially fit for permeability measurement of the three-layer composite membranes was constructed according to Weichart¹⁴ and Huber.¹⁵

RESULTS AND DISCUSSION

Morphology of Plasma Polymer Layers

As demonstrated by the electron micrographs, pinhole-free polymer films of uniform thickness were produced (Fig. 1). In all cases the surface shows hemispherical structures of different sizes and broad size distribution, which are incorporated into the layer (Fig. 2). Similar structures have been observed by Haraguchi and Ide¹⁶ when polymerizing perfluorobenzene in the plasma. For clarity, the structures presented in Figure 2 are somewhat larger than usual.

We did not try to minimize the layer thickness, but from its fluctuations a minimum thickness of 500 nm can be inferred as a cautious estimate.

The polymers are brittle, as may be expected from the fracture surface of some of the polymer films. That means flexible supports will lead to

breakdown and leakage of the adherent plasma polymer layer when the membrane is set under pressure, and for that reason only stiff carriers are suitable. In tetrahydrofuran, which was used to clean the reaction chamber of the polymer residue, the plasma polymers get a certain elasticity because of swelling but they are not dissolved.

Plasma Polymer Composition

Figure 3 depicts the fluorine-to-carbon ratio measured by X-ray analysis versus the mixture ratio of the feed gas. The fluorine content of the plasma polymer increases with the portion of hexafluoroethane in the feed.

The hydrogen-to-carbon ratio determined by quantitative elemental analysis as a function of the feed mixture ratio is represented in Figure 4. As the hydrogen share in the feed gas is reduced, the amount of hydrogen in the depositions decreases.

X-ray photoelectron spectra of plasma polymers produced at different feed gas ratios are shown in Figure 5. Table I gives molar percentages of fluorine-containing carbon groups and the respective C1s binding energies as obtained by deconvolution of the spectra. As predicted by the theory,¹² in general the C1s binding energies are shifted to higher values as the fluorine content of the polymer rises. CF₃ and CF₂ groups become more frequent along with increasing hexafluoroethane content of the feed, whereas the percentage of carbon with fluorine atoms exclusively in secondary positions (C – CF_{n>1}) drops over the whole range of mixture. The CF percentage displays a maximum. The least-fluorinated polymer shows an additional peak attributed to carbon

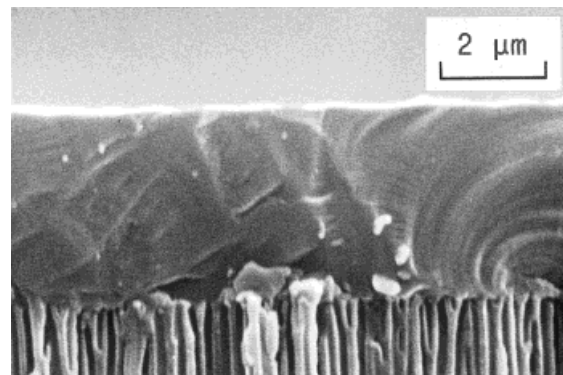


Figure 1 Typical scanning electron micrograph of the fracture surface of a plasma polymer layer on porous aluminium oxide.

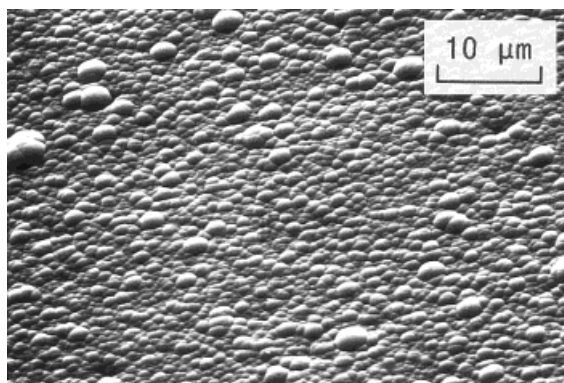
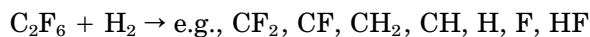


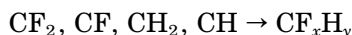
Figure 2 Typical hemispherical structures on the surface of a plasma polymer layer, somewhat larger ($\times 1.5$) than usual.

bound only to carbon and hydrogen, but with only one single secondary fluorine ($C - CF$).

For explanation of the analytical results, a closer look at the reaction mechanism is required. The decomposition of hexafluoroethane/hydrogen mixtures by the electric energy of the plasma entails the generation of numerous radicals and molecules⁴:



Combination reactions of the carbon-bearing radicals result in the deposition of a plasma polymer containing fluorine and hydrogen; for example,



Because the formation and combination of the polymerizable radicals both proceed in accordance with statistical laws, the distributions of fluorine and carbon in the polymerization product resemble their distributions in the feed gas.

After the polymerization process, a varying number of trapped radicals is left unreacted in the deposition. Therefore, atmospheric oxygen will be added to these radical sites on exposing the samples to air.³⁻⁵ The oxygen-to-carbon ratio as stated by X-ray analysis is shown in Figure 6. (These data are confirmed by O1s XPS results not presented.) The oxygen/carbon ratio becomes smaller along the axis of the feed gas mixture ratio, indicating a decrease in concentration of trapped radicals in the fresh polymer. Such a decrease in trapped radical concentration should be accompanied by a drop in crosslink density.

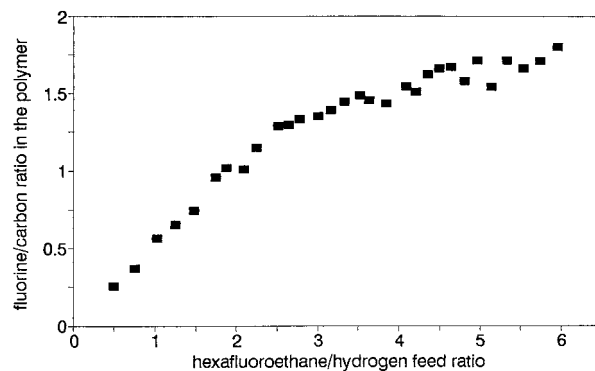


Figure 3 Molar fluorine-to-carbon ratio from X-ray analysis of the plasma polymers as a function of hexafluoroethane-to-hydrogen volume ratio in the feed gas.

Calculation of Crosslink Density

The degree of crosslinking was calculated by means of so-called double-bond equivalents (DBE), being defined as the sum of double bonds and organic cycles in a molecule. DBE can be determined by organic elemental analysis. The point is that each crosslink creates one mesh of the polymer network and therefore can be regarded as an organic cycle. Hence, to obtain the number of crosslinks in a molecule, we merely subtracted the number of actual double bonds from the number of DBE. (The method cannot be applied if organic cycles limited to only one chain are present in the polymer, as for instance if they originate from a monomer already carrying a cyclic structure.)

The number of DBE in a molecule consisting of a number of carbon atoms (C) and, apart from that, only of a number (X) of monovalent atoms (such as hydrogen and halogens, as being the case

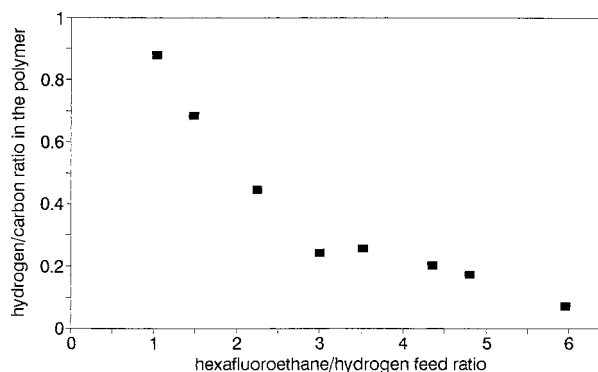


Figure 4 Molar hydrogen-to-carbon ratio from quantitative elemental analysis of the plasma polymers as a function of hexafluoroethane-to-hydrogen volume ratio in the feed gas.

for most of the produced polymers) is calculated as follows:¹⁷

$$DBE = \frac{2C + 2 - X}{2}$$

Bivalent atoms such as oxygen or sulfur, if they occur, do not have to be taken into account. Rearrangement yields

$$\frac{DBE}{C} = 1 + \frac{1}{C} - \frac{X}{2C}$$

In the produced polymers the number X of monovalent atoms is given by the sum of the num-

bers F and H of fluorine and hydrogen atoms, respectively:

$$X = F + H$$

Double bonds are not expected in the polymers because of the presence of hydrogen radicals in the glow discharge. For proof, X-ray photoelectron spectra were scrutinized to trace so-called shake-up satellites shifted to higher binding energies a few eV from the primary C1s peak, which ought to appear in all polymeric systems containing unsaturation.¹² No satellites were found and therefore the existence of double bonds was shut out. Consequently, the number of DBE and the number M of meshes (crosslinks) in the polymer molecule are the same:

$$DBE = M$$

It follows that the number of crosslinks per carbon atom of any saturated network containing solely carbon, fluorine, and hydrogen is given by

$$\frac{M}{C} = 1 + \frac{1}{C} - \frac{F}{2C} - \frac{H}{2C}$$

The numbers of the respective atoms in the polymer molecule are not known. However, atomic ratios can be specified. Considering that the number C of carbon atoms in a highly cross-linked polymer is very large, one may simplify and obtain

$$\frac{M}{C} = 1 - \frac{F}{2C} - \frac{H}{2C}$$

As demonstrated by Figure 7, the increase in crosslink density observed upon raising the hydrogen concentration in the feed parallels the increase in oxygen content but exceeds it by several times. For that reason, the presence of oxygen cannot be the main cause for crosslinking. The simultaneous increase of both crosslink density and oxygen content must result from a rising portion of multifunctional radicals among the polymerizable radicals in the plasma. Multifunctional radicals are probably generated by abstraction of fluorine from hexafluoroethane and its reaction products by hydrogen atoms. In fact, it has been shown by d'Agostino⁴ that where hydrogen feed concentration is high hydrogen atom concentration is likewise high and CF and CH radicals ap-

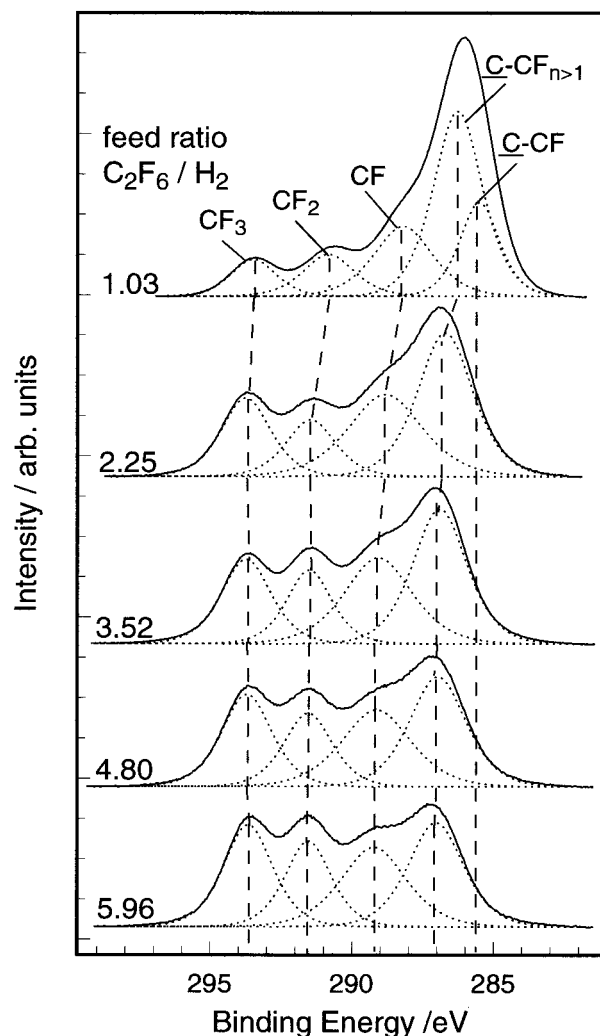


Figure 5 C1s X-ray photoelectron spectra of plasma polymers deposited at different hexafluoroethane-to-hydrogen volume ratios in the feed gas. The respective feed mixture ratio is specified on the left.

Table I Molar Percentages of Fluorine-bearing Carbon Features from X-ray Photoelectron Spectroscopy of Plasma Polymers Deposited at Different Hexafluoroethane/Hydrogen Ratios in the Feed Gas

Feed Ratio C_2F_6/H_2	C – CF	C – CF _{n>1}	CF	CF ₂	CF ₃
1.03	18.0 (285.5)	43.6 (286.3)	20.0 (288.2)	10.4 (290.8)	8.0 (293.5)
2.25	—	38.5 (286.7)	29.3 (288.8)	13.5 (291.5)	18.7 (293.8)
3.52	—	35.3 (286.9)	28.2 (289.1)	16.1 (291.5)	20.4 (293.8)
4.80	—	31.5 (287.0)	26.9 (289.1)	18.0 (291.6)	23.6 (293.7)
5.96	—	28.9 (287.0)	26.1 (289.2)	19.8 (291.5)	25.2 (293.7)

Respective C1s binding energies (eV) are in parentheses.

pear frequently.⁴ These and other multifunctional radicals give rise to the formation of crosslinks, or, in case radical sites are trapped unreacted in the polymer after the plasma process, they will add oxygen on contact with air.

Permeation Properties

The plasma polymers present an increase in oxygen permeability coefficient and in selectivity, but exhibit almost constancy of the nitrogen permeability coefficient upon increase in the hexafluoroethane content of the feed gas (Figs. 8–10). Maximum selectivity is approximately 3.4 at an oxygen permeability coefficient of 21 Barrer and a feed mixture ratio of 5.5. For a simplified discussion of this behavior the idea of a solubility-type

selectivity and a mobility-type selectivity is quite helpful. In the first case the selectivity results from different sorption coefficients, whereas in the second case it ensues from different diffusion coefficients of a gas couple:¹⁸

$$\frac{P(O_2)}{P(N_2)} = \frac{D(O_2)}{D(N_2)} \times \frac{S(O_2)}{S(N_2)}$$

The ratio of the diffusion coefficients is termed “mobility selectivity”; the ratio of the sorption coefficients is the “solubility selectivity.”

The diffusion coefficient of a gas in a polymer depends on the energy of interchain channel formation, which is considered as the activation energy of the diffusion.^{9,10} The larger the gas mole-

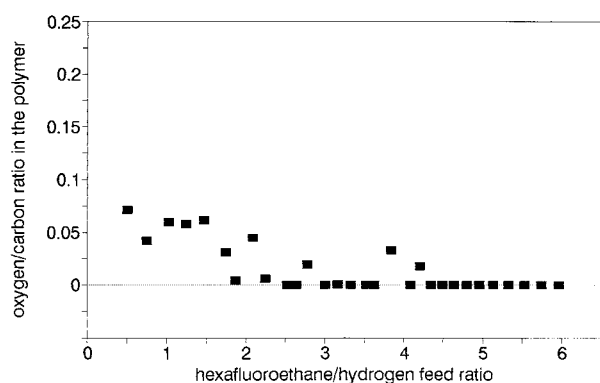


Figure 6 Molar oxygen-to-carbon ratio from quantitative elemental analysis of the plasma polymers as a function of hexafluoroethane-to-hydrogen volume ratio in the feed gas.

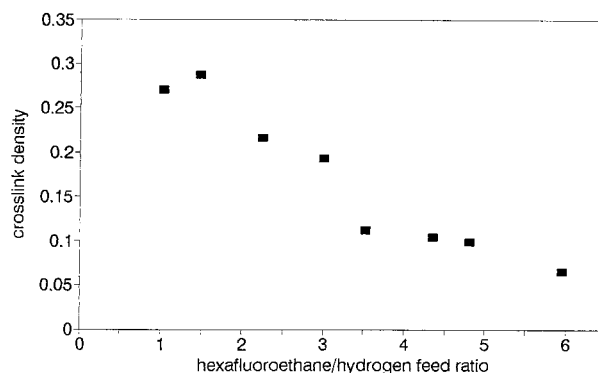


Figure 7 Crosslink density (number of net meshes per carbon atom) of the plasma polymers calculated by X-ray analysis and quantitative elemental analysis as a function of hexafluoroethane-to-hydrogen volume ratio in the feed gas.

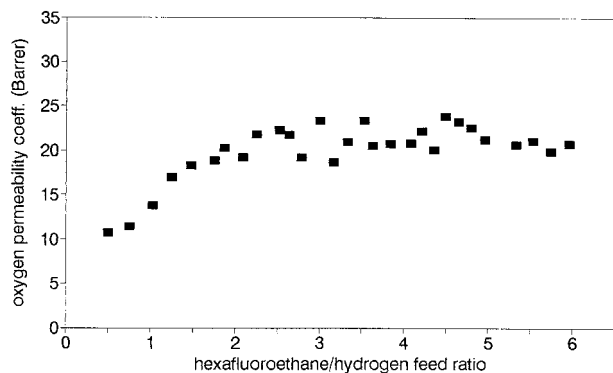


Figure 8 Oxygen permeability coefficient of the plasma polymers as a function of hexafluoroethane-to-hydrogen volume ratio in the feed gas.

cules, the larger are the channels required for the diffusive jumps of the molecules and the larger is the energy needed to form the channel. If the activation energy is increased, that of the bigger penetrant of a gas couple will increase more than that of the smaller penetrant. This will favor the diffusion of the smaller penetrant and entail mobility-type selectivity. On the other hand, any structural change leading to a higher activation energy impedes the diffusion of the smaller penetrant of the gas couple, too. Thus, rising mobility-type selectivity is always accompanied by falling diffusion coefficients and (as long as the sorption coefficients do not grow) by falling permeability coefficients of both gases. As Figure 11 demonstrates for the selectivity and the oxygen-permeability coefficient, the latter is not the case here.

Crosslinking of the plasma polymer chains enhances the activation energy of diffusion,¹⁹ and favors the diffusion of oxygen compared with nitrogen, since the nitrogen molecule is somewhat

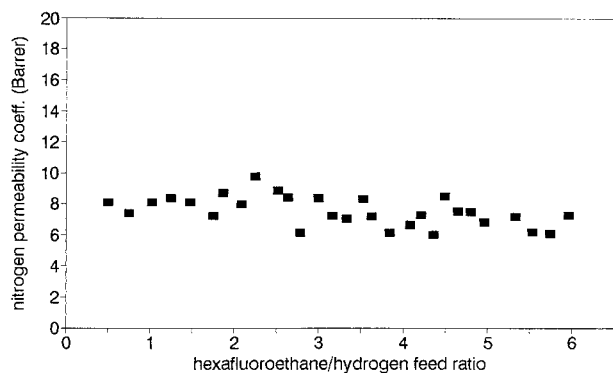


Figure 9 Nitrogen permeability coefficient of the plasma polymers as a function of hexafluoroethane-to-hydrogen volume ratio in the feed gas.

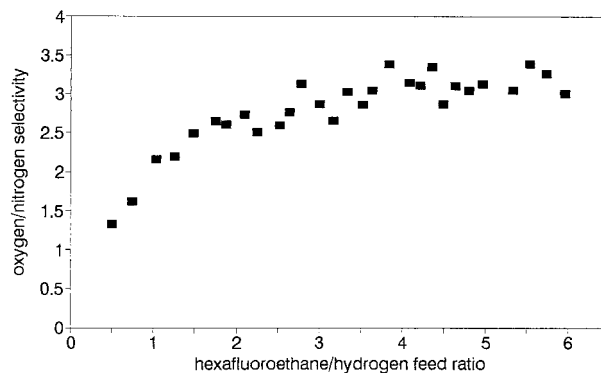


Figure 10 Oxygen/nitrogen selectivity of the plasma polymers as a function of hexafluoroethane-to-hydrogen volume ratio in the feed gas.

bigger (298 nm and 315 nm, respectively).²⁰ However, a change in crosslink density is not the reason for the increasing selectivity of the plasma polymers upon raising the feed mixture ratio because crosslink density drops, not increases.

The introduction of bulky side groups at the polymer chains reduces the coherence between the polymer chains and hence decreases the activation energy of diffusion. Therefore such side groups are expected to cause lower selectivity but higher diffusion coefficients. This has been demonstrated by Hayakawa and colleagues²¹ for the CF_3 structural feature, which is the biggest mon-carbon unit identified in the plasma polymers. According to Hayakawa and associates,²¹ selectivity should grow when CF_3 percentage falls. Since the opposite is valid here, a change in CF_3 percentage cannot be the cause of the observed rise of plasma polymer selectivity either when increasing the hexafluoroethane content of the feed.

From the above, it follows that no evidence of

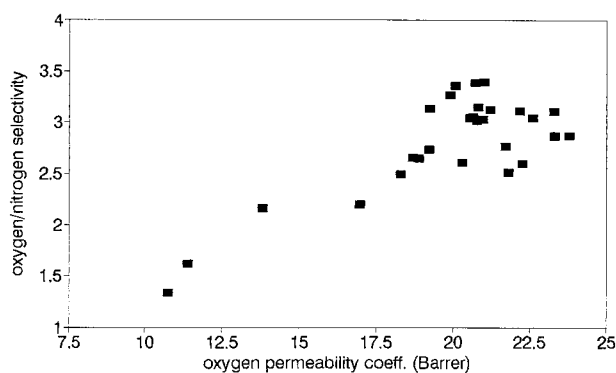


Figure 11 Oxygen/nitrogen selectivity of the plasma polymers as a function of oxygen permeability coefficient.

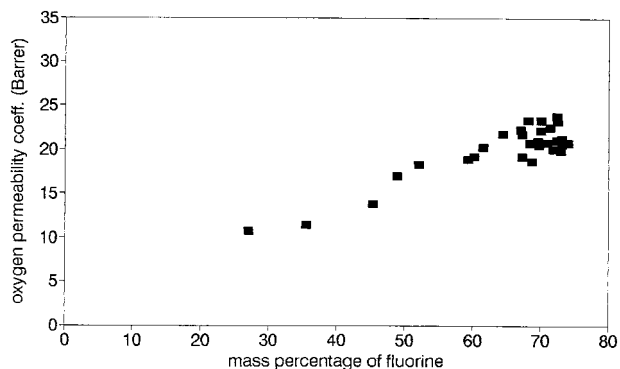


Figure 12 Oxygen permeability coefficient of the plasma polymers as a function of the mass percentage of fluorine contained in the polymers.

mobility-type selectivity can be furnished, and the possibility of solubility-type selectivity should be considered next. In fluorine-containing organic compounds the sorption coefficient for oxygen is usually higher than the sorption coefficient for nitrogen.⁸ The permeability coefficients and the selectivity as a function of the mass percentage of fluorine are presented in Figures 12–14. The oxygen-permeability coefficient and the selectivity show a nearly linear growth with the fluorine content of the polymer, but the nitrogen permeability coefficient remains roughly constant. Besides, it can be seen in Figure 11 that the oxygen-permeability coefficient and the selectivity increase simultaneously, as is typical for solubility-type selectivity.

SUMMARY AND CONCLUSIONS

Pinhole-free plasma polymer layers of an estimated minimum thickness of about 500 nm can

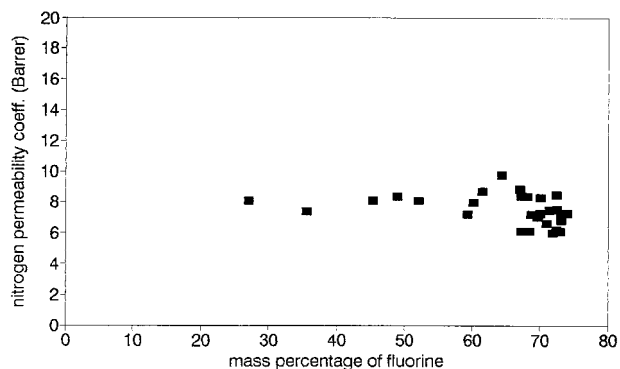


Figure 13 Nitrogen permeability coefficient of the plasma polymers as a function of the mass percentage of fluorine contained in the polymers.

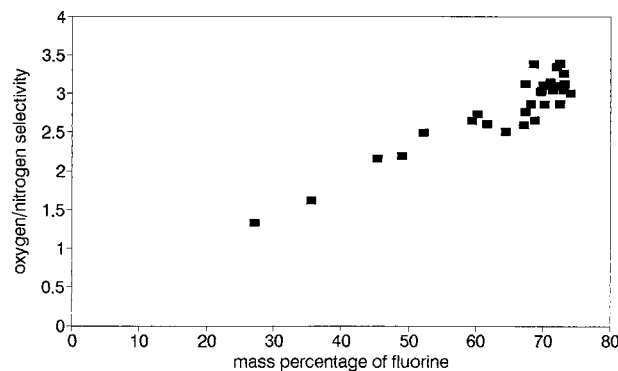


Figure 14 Oxygen/nitrogen selectivity of the plasma polymers as a function of the mass percentage of fluorine contained in the polymers.

be deposited from discharges of hexafluoroethane/hydrogen mixtures. Since the layers are brittle, they have to be applied onto stiff carriers for use in oxygen/nitrogen separation.

The plasma polymers consist of fluorine, carbon, and hydrogen. The distributions of fluorine and hydrogen in the polymers parallel their distributions in the feed. Some of the polymers also contain traces of oxygen, which is from the reaction of trapped radicals with atmospheric oxygen after samples are exposed to air. CF_3 , CF_2 , and CF groups, and carbon structural features exhibiting fluorine only in β -positions have been identified.

Crosslink density can be extracted from DBE determined by elemental analysis because the meshes of the polymer network are organic cycles and actual double bonds are absent.

The maximum selectivity of the plasma polymers is approximately 3.4 at an oxygen permeability coefficient of 21 Barrer. Very likely the rise of selectivity upon increasing the hexafluoroethane content of the feed gas is caused by an increase in solubility selectivity due to the growing fluorine content of the polymers.

The authors gratefully acknowledge the generous financial support of the Deutsche Forschungsgemeinschaft and the Technische Universität Berlin, without which this publication would not have been possible.

REFERENCES

1. A. Gollan and M. H. Kleper, *AIChE Symp. Ser. No. 250*, **82**, 35 (1986).
2. H. K. Lonsdale, *J. Membr. Sci.*, **33**, 121 (1987).

3. H. Biedermann and Y. Osada, *Plasma Polymerization Processes*, Elsevier Science Publishers, Amsterdam, 1992.
4. R. d'Agostino, *Plasma Deposition, Treatment, and Etching of Polymers*, Academic Press, San Diego, 1990.
5. H. Yasuda, *Plasma Polymerization*, Academic Press, Orlando, 1985.
6. A. T. Bell, *Top. Curr. Chem.*, **94**, 43 (1980).
7. V. T. Stannett, W. J. Koros, D. R. Paul, H. K. Lonsdale, and R. W. Baker, *Adv. Polym. Sci.*, **32**, 71 (1979).
8. E. P. Wesseler, R. Iltis, and L. C. Clark, *J. Fluorine Chem.*, **9**, 137 (1977).
9. H. L. Frisch and S. A. Stern, *Critical Reviews in Solid State and Materials Sciences*, Vol. 11, 2nd Ed., CRC Press, Boca Raton, 1983.
10. D. Raucher and M. D. Sefcik, *ACS Symp. Ser.*, **223**, 89 (1983).
11. F. Huber and J. Springer, *J. Appl. Polym. Sci.*, **62**, 165 (1996).
12. D. Briggs and M. P. Seah, *Practical Surface Analysis*, John Wiley & Sons, New York, 1983.
13. J. D. Schultze, Ph.D. Thesis, Technische Universität Berlin, Berlin, 1992.
14. J. Weichart, *Fortschritt-Berichte VDI*, Reihe 3, VDI-Verlag, Düsseldorf 1992, p. 290.
15. F. Huber, Ph.D. thesis, Technische Universität Berlin, Berlin, 1995.
16. T. Haraguchi and S. Ide, *J. Appl. Polym. Sci., Appl. Polym. Symp.*, **42**, 357 (1988).
17. E. Pretsch, T. Clerc, J. Seibl, and W. Simon, *Strukturauflklärung organischer Verbindungen*, 3rd ed., Springer Verlag, Berlin, 1986.
18. R. T. Chern, W. J. Koros, H. B. Hopfenberg, and V. T. Stannett, *ACS Symp. Ser.*, **269**, 25 (1985).
19. C. A. Kumins, *J. Polym. Sci., Part C*, **10**, 1 (1965).
20. R. C. Weast, *Handbook of Chemistry and Physics*, 5th ed., The Chemical Rubber Company, Cleveland, 1970.
21. Y. Hayakawa, M. Nishida, T. Aoki, and H. Muramatsu, *J. Polym. Sci., Polym. Chem. Ed.*, **30**, 873 (1992).